Photochemistry and Photobiology, 2013, 89: 782–791

Numerical Investigation of Upper-Room UVGI Disinfection Efficacy in an Environmental Chamber with a Ceiling Fan†

Shengwei Zhu*[1,2], Jelena Srebric[2], Stephen N. Rudnick[3], Richard L. Vincent[4] and Edward A. Nardell[3,5]

[1]School of Architecture and Urban Planning, Huazhong University of Science and Technology, Wuhan, China
[2]Department of Architectural Engineering, Pennsylvania State University, University Park, PA
[3]Department of Environmental Health, Harvard School of Public Health, Boston, MA
[4]General Internal Medicine, Mount Sinai School of Medicine, New York, NY
[5]Division of Global Health Equity, Brigham and Women's Hospital, Boston, MA

Received 28 September 2012, accepted 21 December 2012, DOI: 10.1111/php.12039

ABSTRACT

This study investigated the disinfection efficacy of the upper-room ultraviolet germicidal irradiation (UR-UVGI) system with ceiling fans. The investigation used the steady-state computational fluid dynamics (CFD) simulations to solve the rotation of ceiling fan with a rotating reference frame. Two ambient air exchange rates, 2 and 6 air changes per hour (ACH), and four downward fan rotational speeds, 0, 80, 150 and 235 rpm were considered. In addition, the passive scalar concentration simulations incorporated ultraviolet (UV) dose by two methods: one based on the total exposure time and average UV fluence rate, and another based on SVE3* (New Scale for Ventilation Efficiency 3), originally defined to evaluate the mean age of the air from an air supply opening. Overall, the CFD results enabled the evaluation of UR-UVGI disinfection efficacy using different indices, including the fraction of remaining microorganisms, equivalent air exchange rate, UR-UVGI effectiveness and tuberculosis infection probability by the Wells–Riley equation. The results indicated that air exchange rate was the decisive factor for determining UR-UVGI performance in disinfecting indoor air. Using a ceiling fan could also improve the performance in general. Furthermore, the results clarified the mechanism for the ceiling fan to influence UR-UVGI disinfection efficacy.

INTRODUCTION

Wells *et al.* (1) first proposed and demonstrated the concept of upper-room ultraviolet germicidal irradiation (UR-UVGI) in 1942. UR-UVGI systems aim to disinfect air with a high irradiation field in the upper portion of the room above occupants' heads. The system typically uses the ultraviolet (UV) fixtures suspended from a ceiling or mounted on a wall. As the sources of infectious microorganisms and susceptible room occupants typically reside in the lower portion of the room with a low UV irradiation field, the vertical movement of room air, which moves the microorganisms from the lower room into the upper room with a high UV irradiation field, is one of the key determinants of UR-UVGI system disinfection efficacy. It is not only important to rapidly transport the microorganisms from the source to the upper room but it is also crucial to have the infectious microorganisms exposed long enough in the upper room to enable inactivation of their DNA. However, lethal exposure can be achieved through one or multiple passes of microorganisms throughout the irradiated zone.

A properly designed, high-volume mechanical ventilation system can control the indoor air movement. However, for most buildings in resource-limited settings, such ventilation systems are often too expensive in terms of installation, operation and maintenance costs. To promote the vertical air movement and rapid transport of the infectious microorganisms to the upper portion of the room, ceiling fans are considered the most appropriate solution to enhance the performance of UR-UVGI systems. Several research groups have found that the operation of a ceiling fan enhances UV inactivation of microorganisms, sometimes with spectacular effects (2–6). A recent report indicated that UR-UVGI with ceiling fans could be 70–80% effective in disinfecting air in a real hospital setting (7). Although ceiling fans appear to be useful in improving the performance of UR-UVGI systems, there are still many unknowns on how best to use ceiling fans to maximize the UR-UVGI air disinfection.

Several studies examined the UR-UVGI system using computational fluid dynamics (CFD) (8–11). However, none of the existing studies included a ceiling fan in the CFD modeling efforts. As a result, this study proposed and validated a CFD modeling method to incorporate the rotation of the ceiling fan's blades with a rotating reference frame (12). The CFD method is available to any kind of ceiling fans, and it is suitable for a parametric investigation of ceiling fans' influence on indoor air mixing and the infection control with UR-UVGI. To save computational time, this method solves the transient phenomenon of the ceiling fan's rotation with the steady-state simulations.

With the aforementioned CFD modeling method, this paper investigated the ceiling fan's influence on UR-UVGI disinfection efficacy for tuberculosis (TB) by changing its downward rotational speed. The investigation used two ambient ventilation conditions: one with an air exchange rate of 2 air changes per hour (ACH) and another with 6 ACH. Overall, this study evaluated UV dose for the microorganisms with two methods, one by multiplying the total exposure time and average UV fluence rate (9), and another based on the simulation of SVE3* (New Scale for

†This paper is part of the Symposium-in-Print on "Ultraviolet Germicidal Irradiation."
*Corresponding author email: szhu@mail.hust.edu.cn (Shengwei Zhu)

Ventilation Efficiency 3) (13), which was originally defined to evaluate the mean age of the air from an air supply opening. In addition, this study also evaluated the UR-UVGI disinfection efficacy using several different indices, including the fraction of remaining microorganisms (5), equivalent air exchange rate (5), UR-UVGI effectiveness (11) and infection probability by Wells–Riley equation (14,15). Advantages and limitations of the modeling and performance evaluation methods are discussed with regard to their proper application to future studies of the optimal use of ceiling fans to improve UR-UVGI disinfection efficacy.

METHODS

This investigation uses CFD methods to account for both convective microorganism transport and their inactivation with an appropriate UV dose set as the sink term in the Eulerian simulation method. The CFD results provide concentration distributions of microorganisms with and without fan and UV fixtures. Finally, these concentration distributions provide inputs into calculations of four different indices to evaluate the UR-UVGI's disinfection efficacy.

CFD model. Environmental chamber model: The room model in Fig. 1 represents the environmental chamber located at the Harvard School of Public Health (5,6). The chamber has a 4.6 m × 2.97 m floor area and a 3.05 m high ceiling about the size of a single-person hospital isolation room. The net volume of indoor space is 41.6 m^3. A ventilation system supplied clean air near the ceiling and exhausted polluted air close to the floor, mixing room air in the process. In addition, clean air was supplied to the room by a ventilation grill that was divided into two nearly equal louvered areas: Fifty-five percent of the area had louvers directing the exiting air parallel to the adjacent wall, and 45% of the grill area had louvers directing exiting air away from the adjacent wall at 30° angle. The ceiling fan (MOD-CAT 20466-300; Hunter Fan Company) was mounted at the center of the ceiling at a height of 2.5 m. A small sphere with the source of a ball-shaped source was located at a height of 1.5 m directly beneath the center of the ceiling fan's motor house. At each corner, there was a 36-W UVGI fixture (Lumalier CM-218) mounted with its bottom surface 2.12 m above the floor. Hence, the UV irradiation field was modeled in a volume between 1.8 and 2.6 m above the floor. In addition, visible light fixtures were mounted to the ceiling and had a total electrical input of 190 W.

Simulation cases: The total number of simulated cases is eight as shown in Table 1. Ambient air exchange rate of 2 and 6 ACH, and fan rotational speeds of 0, 80, 150 and 235 rpm were included in this study. To evaluate the effects of the UV fixtures, each of these cases was simulated with UVGI turned "on" and "off."

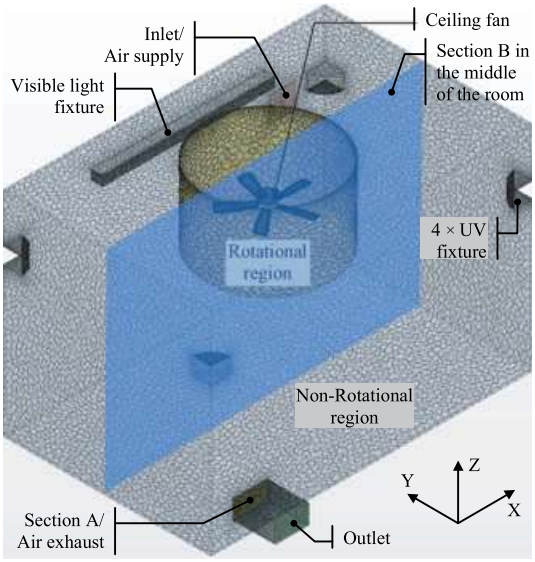

Figure 1. Environmental chamber model in meshes.

Table 1. Simulation cases.

Case	Air exchange rate (ACH)	Downward fan rotational speed (rpm)
1	2	0
2	2	80
3	2	150
4	2	235
5	6	0
6	6	80
7	6	150
8	6	235

CFD methods: This study selected a commercial CFD package, Star-CCM+6.04.014 (16), to create the grid system and perform the simulations.

The simulation field consisted of 1,503,413 spatial cells, among which over 86% was within the rotational region including the ceiling fan to improve the accuracy of the air movement simulations induced by the rotation of fan blades. The prism cell layers were applied to adjust the cell spacing on the wall boundaries, and those along the fan blades were made very thin to ensure sufficient grid resolution to capture the flow characteristics in the near-wall region of the blades as shown in Fig. 2. Overall, a satisfactory grid quality was ensured with the maximum angle skewness under 81° (16).

The realizable k-ε model (17), which was considered more reliable than the standard k-ε model on simulating rotational shear flow, was adopted together with the implicit SIMPLE algorithm (18). Moreover, a two-layer approach (19) using Wolfstein model (20) was used with the all-y^+ wall treatment for the near-wall region, to give the results similar to the low-y^+ treatment for y^+ to be 1 or less, and to the high-y^+ treatment for y^+ >30 (16).For discretizing the governing equations, the finite volume method was applied with the second-order upwind scheme for the velocity components and pressure, and the first-order upwind scheme for the temperature and passive scalars. Furthermore, a rotating reference frame was applied in the rotational region to simulate the fan blades' rotation in a steady state. This method generates a constant grid flux in the appropriate conservation equations by automatically adding the source terms with respect to the Coriolis and Centrifugal forces, which is calculated using the following equation (16):

$$F_r = \rho\omega \times v \quad (1)$$

where Fr is the body force term due to fan rotation (kg m^{-2} s^2), ρ is the air density (kg m^{-3}), ω is the rotational speed (rad s^{-1}) and v is the linear velocity (m s^{-1}).

In Star-CCM+, the global residuals, which are used for judging convergence were normalized by the averages of the first five steps (16). In this study, the continuity and momentum equations were thought to reach convergent when the normalized global residual was less than 1.0 e^{-4}. The convergent level for energy was 5.0 e^{-5}, for scalar terms was 1.0 e^{-6}.

The major boundary conditions are listed in Table 2. The total convective heat transfer at wall surfaces equaled the heat loss due to infrared radiation and conduction from the UV and visible light fixtures (12).

Numerical methods to estimate UV dose. UV dose calculated with exposure time and average UV fluence rate: The UV dose for a microorganism is determined from the strength of UV irradiation field and the microorganism's exposure time to UV irradiation. The exposure time accounts for how long microorganisms remain in the UV irradiation field.

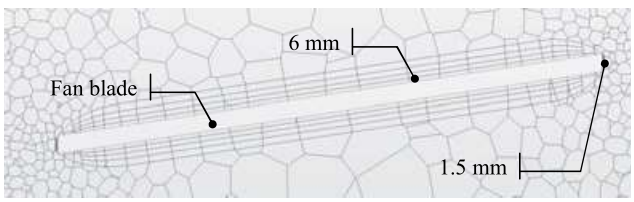

Figure 2. Prism cell layers around the fan blades.

Table 2. Boundary conditions.

Inlet	Size: 0.34 m × 0.34 m; velocity: 0.05 m s^{-1} in Case 1 & 2, 0.2 m s^{-1} in Case 3 & 5 and 0.6 m s^{-1} in Case 4 & 6; temperature: 21.1°C; turbulence intensity: 0.05; turbulence length scale: 0.0016 m
Outlet	Size: 0.48 m × 0.28 m; free slip
UVGI fixtures	No slip; convective heat transfer rate: 48.3 W m^{-2} (10 W per unit)
Visible lamp	No slip; convective heat transfer rate: 50.7 W m^{-2} (totally 57 W)
Source	Diameter: 1 in simulations without source: adiabatic wall, no-slip; in simulations with source: inlet, velocity: 0.012 m s^{-1}; temperature: 21.1°C; turbulence intensity: 0.05; turbulence length scale: 0.00003 m
Ceiling fan	No slip, adiabatic
Walls	No slip, convection heat transfer rate: 1.18 W m^{-2} when UVGI was turned off, and 2.01 W m^{-2} when UVGI was turned on

CFD can provide the microorganism's exposure to the UV irradiation field because the exposure directly depends on the indoor air movement.

Visitation frequency (VF) represents the average number of times the microorganism visited the UV irradiation field (21). VF = 1 means that after being generated, the microorganism visited the UV irradiation field only once. VF = 2 means that after being brought to the UV irradiation field, the microorganism leaves and then returns to the UV irradiation field due to the re-circulating flow for one additional visit.

VF can be obtained from the calculation of the passive scalar flux method. In a room under the steady-state conditions, we can get the following equation by assuming that the rate (a) of the passive scalar flux to return to the UV irradiation field after leaving there is constant.

$$\begin{aligned}\Delta q_{\mathrm{UVi}} &= q_{\mathrm{UVi}}a + q_{\mathrm{UVi}}a^2 + q_{\mathrm{UVi}}a^3 + \ldots + q_{\mathrm{UVi}}a^n + \ldots \\ &= q_{\mathrm{UVi}}a(1 + a + a^2 + \ldots + a^{n-1} + \ldots)\end{aligned} \tag{2}$$

where Δq_{UVi} is the inflow flux of passive scalar into the UV irradiation field (kg s^{-1}) and q_{UVi} is the total generation rate of passive scalar in the UV irradiation field (kg s^{-1}). When $n \to \infty$, the following equation can be established:

$$1 + a + a^2 + \ldots + a^n = (1 - a^n)/(1 - a) = 1/(1 - a) \tag{3}$$

Hence, the rate a can be calculated by Eq. (4) derived from Eqs. (2) and (3).

$$a = \Delta q_{\mathrm{UVi}}/(q_{\mathrm{UVi}} + \Delta q_{\mathrm{UVi}}) \tag{4}$$

As VF equals $1/(1 - a)$, VF can be calculated using the following equation obtained by substituting Eq. (4) into Eq. (3).

$$\mathrm{VF} = 1 + (\Delta q_{\mathrm{UVi}}/q_{\mathrm{UVi}}) \tag{5}$$

In the simulations, the total generation rate was arbitrarily set to be 0.01 kg s^{-1} because Eq. (5) uses the non-dimensional ratio of Δq_{UVi} and q_{UVi} to calculate VF. Specifically, this passive scalar was assumed to be uniformly generated at a rate of 0.001 kg m^{-3} s in the UV irradiation field with a volume of 10 m^3, resulting in a total of 0.01 kg s^{-1}. This volume source, covering the irradiation field, enables calculations of visitation frequency as a performance indicator that couples the performances of the ventilation system and the UV lamps. Therefore, this indicator enables direct performance comparisons for different ventilation and UV lamp systems independent of the actual point source location.

Local purging flow rate (L-PFR) is an index of ventilation efficiency in any specified domain, originally defined as the effective airflow to remove or purge a contaminant from the domain (22). As shown in Eq. (6), L-PFR is defined as the net ventilation rate of the UV irradiation field with the microorganism generation rate (q_{UVi}) and its averaged concentration (C_{UVi}). With this definition, the value of L-PFR can simply be calculated from the microorganism concentration simulations based on the passive scalar transport equation (23).

$$\text{L - PFR} = q_{\mathrm{UVi}}/C_{\mathrm{UVi}} \tag{6}$$

where L-PFR is the local purging flow rate (m^3 s^{-1}); C_{UVi} is the average microorganism concentration in the UV irradiation field (kg m^{-3}).

In addition, as expressed in Eq. (7), L-PFR has a close relation with VF and the average staying time can be calculated using L-PFR and VF.

$$\text{L - PFR} = V_{\mathrm{UVi}}/(\mathrm{VF} \times T_{\mathrm{UVi}}) \tag{7}$$

V_{UVi} is the volume of the UV irradiation field (m^3) and T_{UVi} is the average staying time for the microorganism in the UV irradiation field, which is defined by calculating the average exposure time per visit to the UV irradiation field (s).

By assuming that the UV irradiation field is uniformly irradiated, UV dose for the microorganism can be calculated as:

$$D = I_{\mathrm{AVE}} \times T_{\mathrm{T-UVi}} = I_{\mathrm{AVE}} \times (\mathrm{VF} \times T_{\mathrm{UVi}}) \tag{8}$$

where D is the UV dose (J m^{-2}), $T_{\mathrm{T-UVi}}$ is the total exposure time of the microorganism to the UV irradiation field (s) and I_{AVE} is the average UV fluence rate of the UV irradiation field (W m^{-2}), which was 0.15 W m^{-2}.

The UV dose D accounts for all of the air supplied to the environmental chamber, including the air from the inlet and source, as well as the total exposure time. In addition, the UV dose D is equal to the UV dose at the exhaust in a well-mixed room because it tracks the air from entering to leaving the room.

UV dose calculated with the distribution of UV fluence rate: With Eq. (9), the UV dose can be calculated by considering the effect of the spatial distribution of UV fluence rate. In this method, the UV fluence rate distribution is applied in the UV irradiation zone as scalar fluxes. The UV dose at a specific point is the summation of the UV fluence rate multiplied by the residence time at each point on the air pathway from the air supply, which opens through the point of interest. In addition, because the UV fluence rate is zero outside the UV irradiation zone, the product of UV fluence rate and the residence time will also be zero at any point out of the UV irradiation zone.

$$\frac{\partial D}{\partial t} + \frac{\partial}{\partial x_j}(D \cdot u_j) = \frac{\partial}{\partial x_j}\left((\lambda + \lambda_t)\frac{\partial D}{\partial x_j}\right) + E \tag{9}$$

where u_j is the velocity components (m s^{-1}), λ is the molecular diffusivity (m^2 s^{-1}), λ_t is the kinematic diffusivity (m^2 s^{-1}), and E is the UV fluence rate (W m^{-2}). In this simulation, the spatial distribution of UV fluence rates within the UV irradiation field was obtained from the commercially available Computer-Aided Design (CAD) tool of Visual™ by Acuity Brand Lighting (24). And an interpolation function by Star-CCM+(16) was applied to map the UV fluence rate distribution from the CAD tool onto the CFD grid. Figure 3 provides the fluence rate distribution at the horizontal section 2.2 m above the floor after applying the interpolation procedure. The average UV fluence rate of the UV irradiation field was 0.15 W m^{-2}.

As the air mass at any point of interest consists of the air fractions both from the air supply and source in the room, the UV dose by Eq. (9) is for all of the air fractions at the point. To obtain the spatial distribution of UV dose only for the airborne microorganisms from the source, Kato *et al.* proposed a CFD method based on the concept of SVE3* (New Scale for Ventilation Efficiency) (13). By this method, first the mass ratio (r) of air fraction from the source at each spatial point can be calculated with SVE4 (25) by treating the source as an air supply opening with Eq. (10). r was set to be 1 for the airflow from the source.

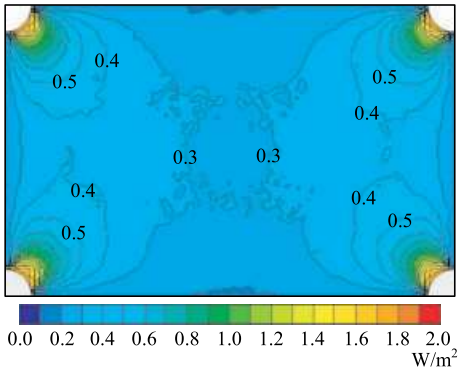

Figure 3. UV fluence rate distribution in the horizontal section 2.2 m above the floor.

$$\frac{\partial r}{\partial t}+\frac{\partial}{\partial x_j}(r\cdot u_j)=\frac{\partial}{\partial x_j}\left((\lambda+\lambda_t)\frac{\partial r}{\partial x_j}\right) \tag{10}$$

Then, the spatial distribution of UV dose for the microorganism can be obtained by dividing the result of Eq. (11) by the mass ratio (r).

$$\frac{\partial Dr}{\partial t}+\frac{\partial}{\partial x_j}(Dr\cdot u_j)=\frac{\partial}{\partial x_j}\left((\lambda+\lambda_t)\frac{\partial Dr}{\partial x_j}\right)+r\cdot E \tag{11}$$

Numerical indices to evaluate UR-UVGI disinfection efficacy. This investigation uses the following indices to evaluate the UR-UVGI disinfection efficacy: the fraction of remaining microorganisms, equivalent air exchange rate, UR-UVGI effectiveness, and infection probability of M.TB by Wells–Riley equation. These indices are calculated based on the results of the passive scalar simulations accounting for the inactivation of the microorganisms.

Passive scalar method for inactivation of microorganisms: The inactivation of the microorganisms by UV irradiation can be coupled in the passive scalar transport equation by adding a source term corresponding to the disinfection of microorganisms as follows (8):

$$\frac{\partial \phi}{\partial t}+\frac{\partial}{\partial x_j}(\phi\cdot u_j)=\frac{\partial}{\partial x_j}\left((\lambda+\lambda_t)\frac{\partial \phi}{\partial x_j}\right)-ZE\phi \tag{12}$$

where ϕ is the concentration of the microorganism (cfu m^{-3}) and Z is the UV susceptibility constant of M. TB (m^2 J^{-1}). The distribution of fluence rate was same as that used in Eq. (9). ($-ZE\phi$) is the source term in the equation, which accounts for the disinfection of microorganisms. The smallest UV susceptibility constant of M. TB (0.23 m^2 J^{-1}) was adopted to evaluate the highest TB infection risk (26).

Fraction of remaining microorganisms and equivalent air exchange rate: Under steady-state condition, the fraction of remaining microorganisms is defined as the ratio of the steady-state concentration of airborne microorganisms with the UVGI turned "on" to the steady-state concentration with the UVGI turned "off" (5). In this study, the calculation of the fraction of remaining microorganisms used the room average concentrations. While calculating the fraction of remaining microorganisms, the concentration of M.TB at the source was assumed to be 1 cfu m^{-3}. Therefore, the results show the fraction of airborne surviving microorganisms after the application of UVGI, inherently including the effects of the HVAC system, ceiling fan, and UR-UVGI system. Its value varies in the range of 0–1, and the closer to zero the fraction of remaining microorganisms is, the better the UR-UVGI disinfection performance indicates. With the fraction of remaining microorganisms, the equivalent air exchange rate (λ_e) attributable to UVGI is defined as the increase in air exchange rate that is required to give the same microorganism concentration without using UVGI, if the space is assumed to be well mixed and under a steady-state condition (5). The equation for calculating λ_e is given as:

$$\lambda_e=\frac{(1-f_{SS})}{f_{SS}}\lambda \tag{13}$$

λ is the ambient air exchange rate (ACH) and f_{ss} is the fraction of remaining microorganisms that survived in the room (–), which was the ratio of the volume averaged concentration of airborne microorganisms with the UVGI turned "on" to the one with the UVGI turned "off" in this study.

UR-UVGI effectiveness: To simultaneously account for the effect of both the indoor air mixing condition and the strength of UR-UVGI lamps, a new non-dimensional parameter, UR-UVGI effectiveness (11), was proposed using the definition of the contaminant removal effectiveness (27).

$$\eta_{UR-UVGI}=1-\frac{1}{\varepsilon'}\cdot\frac{C_{ex-UV}}{\langle C\rangle_{noUV}},\quad \varepsilon'=\frac{C_{ex-nouv}-C_S}{\langle C\rangle_{noUV}-C_S} \tag{14}$$

where $\eta_{UR\text{-}UVGI}$ is the UR-UVGI effectiveness (–); ε' is the contaminant removal effectiveness (–); $C_{ex\text{-}UV}$ is the concentration at the exhaust with UVGI "on" (cfu m^{-3}), $C_{ex\text{-}noUV}$ and $\langle C\rangle_n$oUV are the concentration at exhaust and room average concentration, respectively, with UVGI "off" (cfu m^{-3}), and C_S is the concentration in the air supply (cfu m^{-3}). C_S was zero in our CFD model as the microorganism was only generated from the source. $\eta_{UR\text{-}UVGI}$ also varies from 0 to 1; however, contrary to the fraction of remaining microorganisms, the closer to one $\eta_{UR\text{-}UVGI}$ is, the better the UR-UVGI disinfection effect is.

Infection probability of M.TB by Wells–Riley equation: The probability of airborne TB infection can be predicted by applying the Wells–Riley equation (14,15) with CFD results of microorganism concentration field (28):

$$P=1-e^{-pNt} \tag{15}$$

where P is the infection probability; p is the breathing rate (m^3 s^{-1}); N is the concentration of quanta (quanta m^3), which is the infectious dose of the microorganisms; t is the total exposure time that an occupant is exposed in the air mixed with the infectious microorganisms (s).

In this study, a passive scalar was adopted to represent the M.TB quanta, and the airborne transport of M.TB was calculated with Eq. (12). However, the unit of the scalar concentration was quanta m^{-3} when calculating the infection probability. Furthermore, the generation rate of the infection quanta of M. TB was assumed to be 1 quanta h^{-1} at the source (29).

RESULTS

The indoor velocity distribution and the flow pattern of air from the source will be reported first, followed with the simulation results of the UV dose and the indices for evaluating the UR-UVGI disinfection efficacy, which resulted from the passive scalar simulation based on indoor flow field.

Indoor air mixing

Velocity distribution. Figure 2 shows the vector velocity distribution in the cases with the air exchange rate of 2 ACH. According to Fig. 4, in the simulated small room, the fan was the primary momentum source to form the indoor flow field and completely changed the mixing conditions of room air, even with a low fan rotational speed. The use of a ceiling fan generated air circulation between the side walls and fan-induced airflows, with eddies along the fan-induced airflow and near the floor. In addition, as the fan blades had a pitch of 10.5°, with the increase of the fan rotational speed, the strengthened fan-induced airflows were deflected off each other and small air circulation generated between the fan-induced airflows. The increase of the fan rotational speed enhanced the small air circulation, which finally

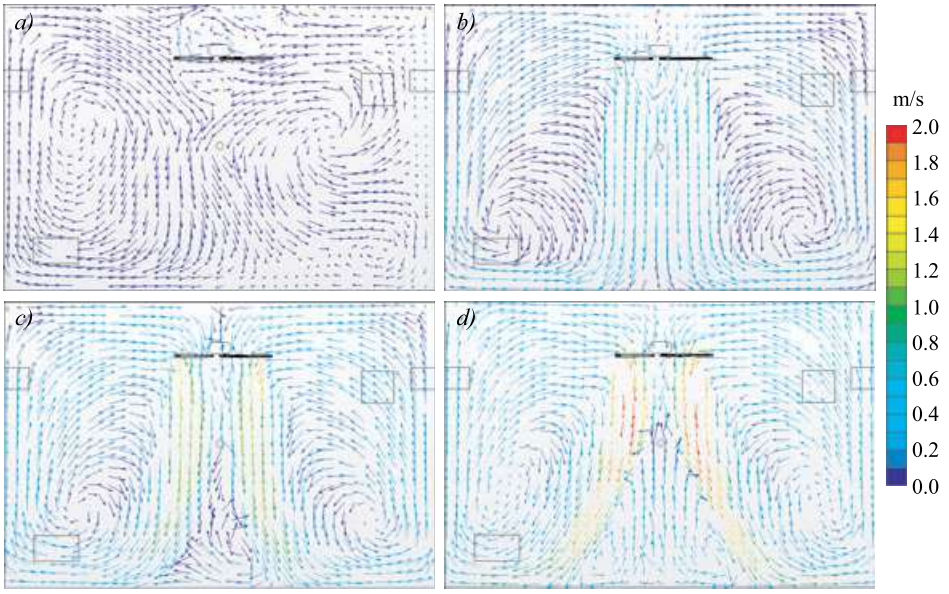

Figure 4. (a–d) Vector velocity distribution in the middle section at *Y*-direction (see Section B in Fig. 1) in the cases with 2 ACH. (a) In Case 1, (b) In Case 2, (c) In Case 3, (d) In Case 4.

affected the local flow field around the microorganism source. A similar phenomenon was found with the air exchange rate of 6 ACH.

Flow pattern of air from the source. Figure 5 illustrates the airflow pattern from the microorganism source in each simulated case. Both the ambient air exchange rate and fan speed had great influence on the airflow pattern. The large air exchange rate reduced the room residence time for the air, as well as the chance to enter the UV irradiation field. In addition, according to Fig. 5(c), in the case with a fan speed of 150 rpm and air exchange rate of 2 ACH, the air from the source was caught in the eddy between the fan-induced airflow and left side wall, and that contaminated air was unable to escape from the eddy to reach the upper irradiated zone.

Mass flow rate of the air entering UV irradiation field. Figure 6 shows the change of the mass flow rate of the air that entered the UV irradiation field as a function of fan rotational speed. It indicates that the use of a ceiling fan significantly promoted the vertical air movement as expected with the increase in the fan rotational speed. Moreover, counter intuitively, ceiling fan's influence on vertical air mixing was independent of the air exchange rate when it was in the range of 2–6 ACH.

UV dose

Table 3 summarized and compared VF, total exposure time and the UV dose calculated by two methods in each case.

VF and exposure time. According to Table 3, for the same air exchange rate, VF increased with the fan rotational speed, while the average exposure time decreased. Furthermore, for the same fan rotational speed, VF increased about three times when the air exchange rate was reduced from 6 to 2 ACH and the average exposure time changed very slightly. Therefore, the total exposure time was inversely proportional to the air exchange rate. However, again counter intuitively, the total exposure time varied slightly with the fan rotational speed, while the air exchange rate was not changed.

UV dose at the exhaust. In Table 3, the UV dose was first calculated by multiplying the total exposure time and the average UV fluence rate ($D_{UV\text{-}1}$). Furthermore, the UV dose was also calculated by using SVE3* ($D_{UV\text{-}2}$). As aforementioned, $D_{UV\text{-}1}$ also represented the UV dose at the exhaust. According to Table 3, $D_{UV\text{-}1}1$ was slightly larger than $D_{UV\text{-}2}$ in each case because $D_{UV\text{-}1}$ was calculated for all of the supplied air, while $D_{UV\text{-}2}$ was calculated for air only from the microorganism source. Similar to the total exposure time, both $D_{UV\text{-}1}1$ and $D_{UV\text{-}2}$ were inversely proportional to the air exchange rate, with their values for 2 ACH being around three times of those for 6 ACH.

UV dose distribution. Figure 7 shows the UV dose distribution calculated by SVE3* in the cases with the air exchange rate of 2 ACH. As intended, the UV dose was larger in the upper room than in the lower space following the gradient in UV fluence. UV dose gradient was apparently greater in Case 1, and it became uniform in other cases as the vertical air movement was promoted by the ceiling fan. The higher the fan rotational speed was, the more uniform the dose distribution was. Furthermore, the UV dose showed a relatively symmetrical distribution in the vertical section when using a ceiling fan. Similar results were obtained when the air exchange rate was 6 ACH. However, the UV dose reduced to around one-third, which is consistent with the results at the exhaust as shown in Table 3.

UR-UVGI disinfection performance

The UR-UVGI disinfection performance in each case is examined and compared in terms of the fraction of remaining microorganisms, equivalent air exchange rate, UR-UVGI effectiveness and TB infection probability.

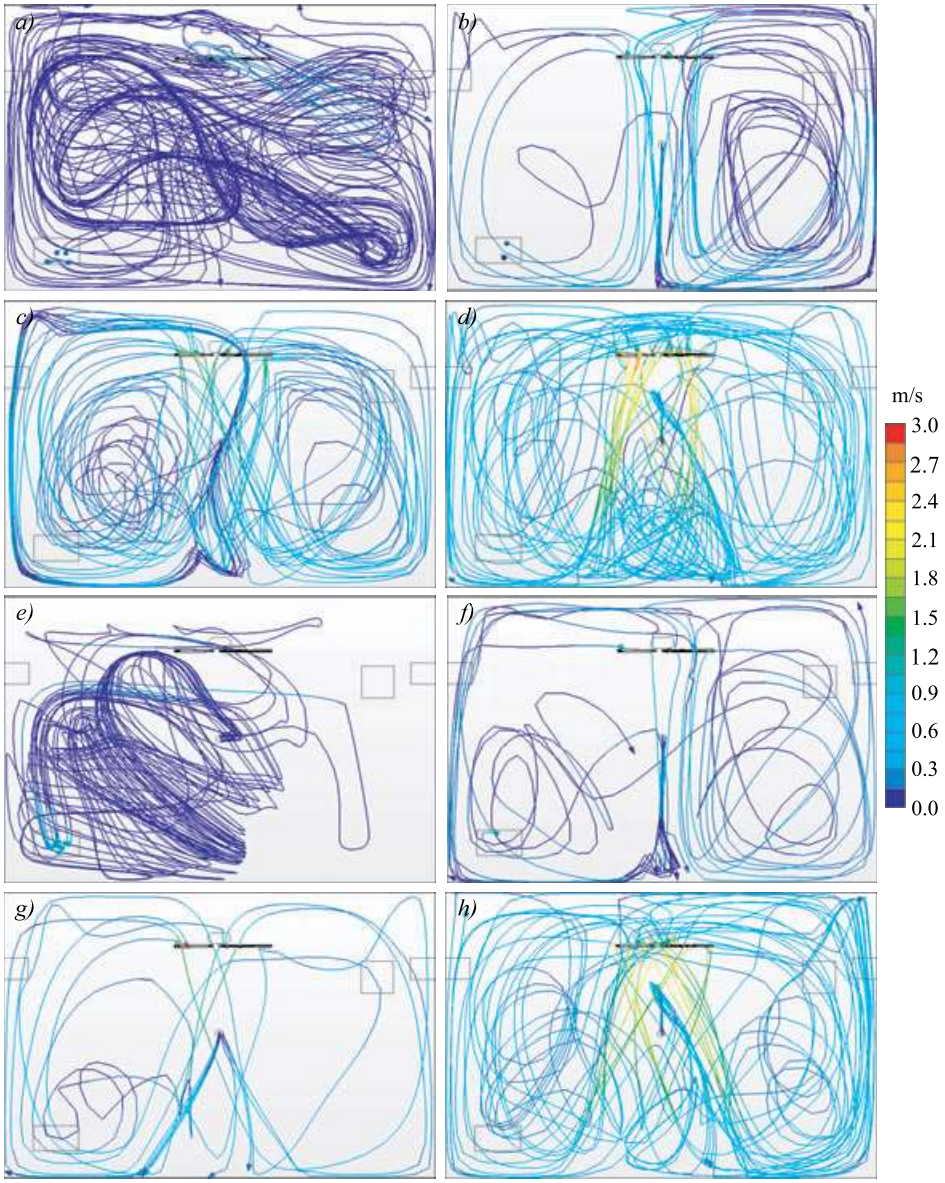

Figure 5. (a–h) Streamline of air from the source in the middle section at *Y*-direction (see Section B in Fig. 1) in the Cases 1–8. (a) In Case 1, (b) In Case 2, (c) In Case 3, (d) In Case 4; (e) In Case 5, (f) In Case 6, (g) In case 7, (h) In Case 8.

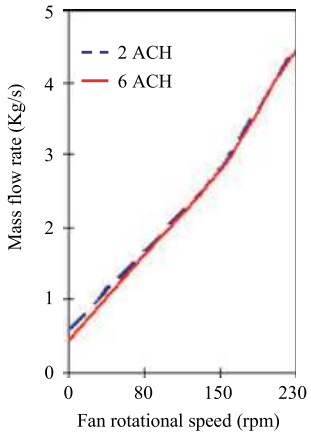

Figure 6. Relation between mass flow rate of air entering UV irradiation field and fan rotational speed.

Table 3. Summary of CFD estimation of UV dose.

Case	Average exposure time (s)	VF (–)	Total exposure time (s)	UV dose by total exposure time & average UV fluence rate (J m^{-2})	UV dose by SVE3* at exhaust (J m^{-2})
1	21.0	21	441	64.5	60.5
2	7.8	56	437	63.8	61.7
3	4.6	97	446	65.0	64.0
4	2.9	151	438	63.8	63.2
5	23.4	6	140	20.9	20.2
6	7.6	19	148	22.1	20.3
7	4.5	33	149	21.7	20.7
8	2.9	52	151	21.6	21.0

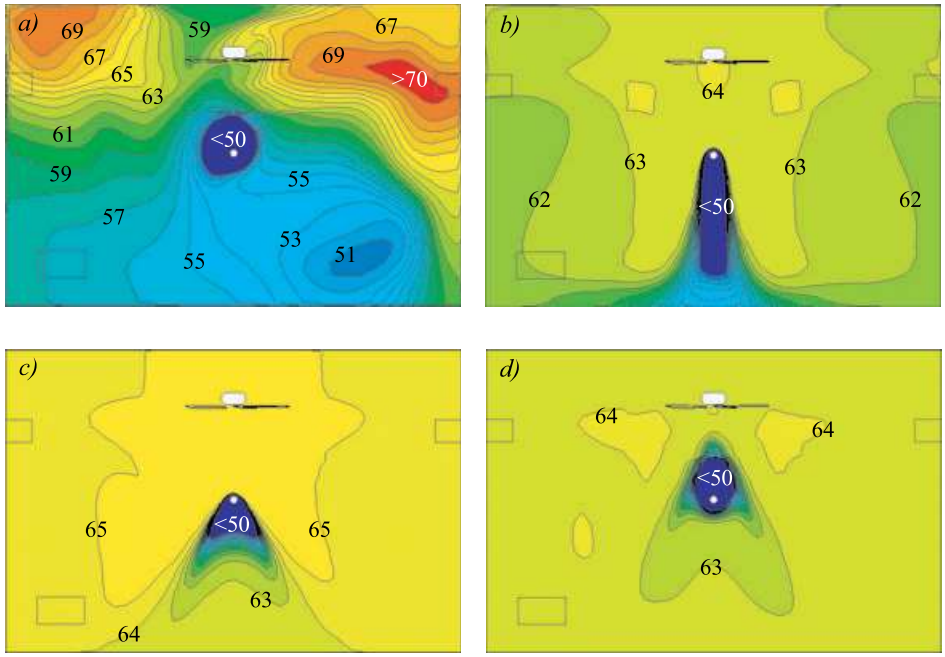

Figure 7. (a–d) Distribution of UV dose in the middle section at *Y*-direction (see Section B in Figure 1) in the cases with 2 ACH. (a) In Case 1 (b) In Case 2, (c) In Case 3, (d) In Case 4.

Fraction of remaining microorganisms. According to Table 4, with the same fan speed, the fraction of remaining microorganisms was smaller for the small air exchange rate (2 ACH). Furthermore, the fraction of remaining microorganisms decreased when using ceiling fan with the same air exchange rate. In addition, the fraction of remaining microorganisms slightly decreased with the increase of fan rotational speed when the air exchange rate was 6 ACH. However, with the air exchange rate of 2 ACH, the fraction of remaining microorganisms was greatly affected by the fan rotational speed, so it was lowest at the fan speed of 150 rpm and highest at the fan speed of 235 rpm. The result indicated that the fan-induced airflow acted as a much more important factor on UR-UVGI disinfection efficacy when the ambient air supply rate was small.

Equivalent air exchange rate. As shown in Table 4, with the ambient air exchange rate of 2 ACH, the equivalent air exchange rate changed significantly with the fan rotational speed. The equivalent air exchange rate had a maximum value of 57 ACH at a medium fan speed of 150 rpm. For the ambient air exchange rate of 6 ACH, the equivalent air exchange rate varied slightly around 20 ACH.

Table 4. Summary of CFD investigation of UR-UVGI's disinfection efficacy.

Case	Fraction remaining (–)	Equivalent added ACH	Contaminant removal effectiveness (–)	UR-UVGI effectiveness (–)	Infection probability (%)
1	0.160	10.5	1.01	0.876	0.89
2	0.080	23.1	1.02	0.897	0.44
3	0.034	57.0	1.02	0.969	0.35
4	0.124	13.0	1.01	0.867	0.53
5	0.449	7.4	0.97	0.621	0.76
6	0.232	19.9	1.04	0.725	0.37
7	0.223	20.9	1.04	0.791	0.35
8	0.218	21.5	1.03	0.749	0.48

UR-UVGI effectiveness. Because the contaminant removal effectiveness was similar in each case with the values around 1 (Table 4), the indoor air could be considered to be perfectly mixed. However, UR-UVGI effectiveness was higher for the smaller air exchange rate. In addition, according to the results, with the same air exchange rate, the UR-UVGI effectiveness could be improved using ceiling fans with the highest effectiveness for the medium fan with a speed of 150 rpm. This improvement indicated a greater air exchange rate of 6 ACH.

Infection probability. Figure 6 shows the TB infection probability as a function of time in each case with UVGI being "on" and "off," respectively. The infection probabilities were calculated with the surface average concentration at the horizontal plane elevated 1.5 m above the floor, representing the height of the breathing field. In addition, the breathing rate was set to be 8 L min^{-1} (30).

According to Fig. 8, when UVGI was turned "off," the infection probability could be decreased by increasing the air exchange rate. Nevertheless, the infection probability could also be, counter intuitively, increased by the use of the ceiling fan. When the air exchange rate was 2 ACH, the fan rotational speed showed great effect on infection probability with the highest infection probability at the medium fan speed of 150 rpm. When the air exchange rate was 6 ACH, the infection probability increased slightly with the use of the ceiling fan and it was the highest for the fan speed of 235 rpm.

Figure 8 indicated that UR-UVGI significantly decreased the infection probability, especially in the cases with the air exchange rate of 2 ACH that had much higher infection probabilities when UVGI was turned "off." This finding supports the experiential knowledge that ceiling fans can support the disinfection efforts

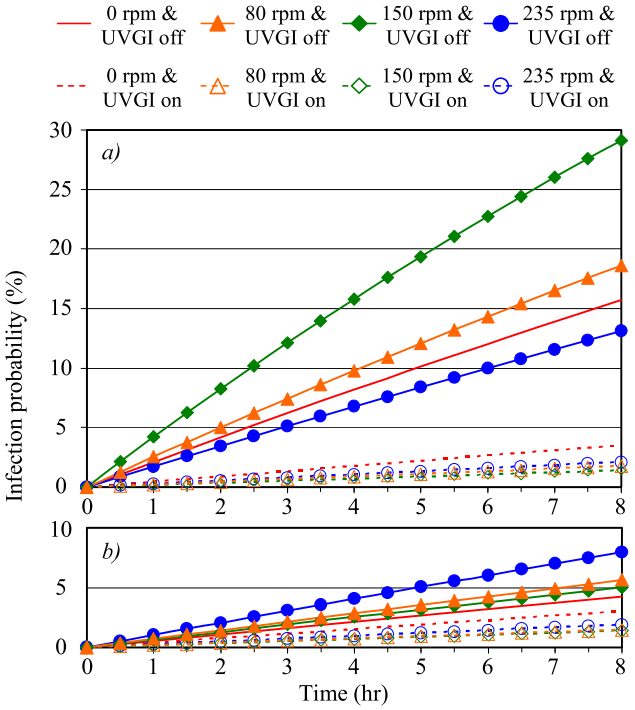

Figure 8. (a–b) Infection probability of TB as a function of time in each case with UVGI "on" and "off".(a) Results of Cases 1–4 with air exchange rate of two ACH; (b) Results of Cases 5–8 with air exchange rate of 6 ACH.

with UR-UVGI, especially for poorly- or non-ventilated spaces. In addition, Table 4 presents the infection probabilities after 2 h of exposure. The infection probability was smaller when using ceiling fan and UR-UVGI together compared with the probability for the system using only UR-UVGI. Furthermore, with the same air exchange rate, the infection probability was smallest at the medium fan speed of 150 rpm.

DISCUSSION

Ceiling fan's influence on the UR-UVGI disinfection efficacy

The simulation results show that the air exchange rate by air supply ventilation was a decisive factor for UR-UVGI performance as the amount of the exposure to UV irradiation was primarily determined by the air exchange rate. The use of a ceiling fan made only a slight difference for the total exposure. This may be in part because the small chamber ventilation rate produced substantial air mixing. In other words, the potential for UVGI to contribute to air disinfection is greatest under low air exchange rate conditions. However, UR-UVGI's ability to disinfect air improved by using the ceiling fan because the ceiling fan transferred the airborne microorganisms from the source to the UV irradiation field much more rapidly. In addition, the use of a ceiling fan also reduced the time for the airborne microorganisms to stay in the UV irradiation field during each visit, and much more frequently sent them to the lower occupied room space, but also briefly. It is conceivable that with a sufficiently high fan speed, the airborne microorganisms had a higher probability to be inhaled before they were inactivated or killed. However, the benefits of effective air disinfection clearly outweigh the risks of using UR-UVGI without an air mixing fan. This is also the likely reason that UR-UVGI disinfection efficacy was highest at the medium fan speed. Therefore, it is important to optimize the operation of the ceiling fan to maximize the UR-UVGI disinfection efficacy.

The simulation results indicated the possibility of exacerbating the risk of airborne infection using ceiling fan in such a small room space if UR-UVGI was turned "off." As ceiling fans are widely used to achieve thermal comfort, it is important to understand that ceiling fans have the potential to distribute risk in the absence of air disinfection, such as UR-UVGI or good ventilation, natural or mechanical.

Examination of the methods to estimate the UV dose

It is much easier to calculate the UV dose by multiplying total exposure time and average UV fluence rate because it overlooks the spatial distribution of fluence rate and only requires one passive scalar transport simulation. In addition, as this method calculates VF and the exposure time at the same time when calculating the UV dose, it is possible to investigate the mechanisms by which the ceiling fan can affect the UV dose. However, this method has three limitations:

1. it cannot predict the distribution of the UV dose and represents only the UV dose at the exhaust, *e.g.* the total UV dose for the supplied air;
2. it ignores the UV fluence rate's distribution which might greatly vary in the upper room;
3. it neglects the microorganism concentration distribution in the air which might be great in a room with poor mixing conditions, and can only estimate the UV dose for all of the supplied air;

The studies on infection control assume that the microorganisms released into the room would come from the patients' cough. However, this method calculates UV dose for the airflow resulting from both the air supply diffusers and the patients' cough. Therefore, it has the potential to overestimate the UV dose even in perfectly mixed conditions. In addition, this method cannot correctly estimate the UV dose in an indoor environment with a poorly mixed condition, where the microorganisms' dispersion is inevitably influenced by the patients' cough, furniture and thermal plumes from heat sources. Therefore, the method to calculate the UV dose by SVE3* is a better solution to estimate the UV dose because it successfully fixes all the problems aforementioned. It can also be applied in any type of indoor ventilation conditions.

Examination of the indices to evaluate the UR-UVGI disinfection efficacy

The fraction of remaining microorganisms is the most commonly used to evaluate the UR-UVGI disinfection efficacy. As almost all of the experimental studies applied mixing ventilation, it was convenient to deploy this index by measuring the concentration at the exhaust (5,6). Since it is easy to calculate the room average concentration with CFD results, the use of this index can be extended to the indoor settings with various ventilation systems. In addition, the equivalent air exchange rate is effective in evaluating the UR-UVGI disinfection efficacy. However, it is only available for the perfectly mixed conditions which assume that the microorganisms are uniformly distributed in the air.

UR-UVGI effectiveness established the relationship between the UR-UVGI disinfection efficacy and the indoor air mixing conditions, therefore enabling different ventilation system effectiveness to be taken into account. As shown in this study, the completeness of air mixing was almost the same in each case as evidenced by the similar contaminant removal effectiveness. However, the UR-UVGI effectiveness varied with the method of air mixing. These results can help to maximize the performance of UR-UVGI by applying the proper air exchange rate and fan downward rotational speed.

The above three indices were developed for evaluating the UR-UVGI disinfection efficacy in the whole room space. These indices can account for the effects of the local indoor settings such as the number and location of microorganism sources, the existence of heat sources and the spatial configuration. But these indices cannot investigate the influence of each contributing parameter in detail. In addition, these indices are unable to evaluate the effects of UR-UVGI on the risk of airborne infection, which is the main aim of modeling. Applying the Wells–Riley equation to estimate the infection probability by using CFD results as input, makes it possible to do the aforementioned parametric investigation of a ceiling fan's influence on UR-UVGI performance with both overall and local infection probabilities. However, it should be noted that the infection probability by the method using Wells–Riley equation, depended on the assumptions of microorganism susceptibility, exposure time and occupant condition. Moreover, as the CFD model simply represented the airborne microorganisms with a passive scalar, and neglected the reduction of the microorganisms due to the particles' deposition and natural death, the simulation results are more useful for a qualitative investigation.

CONCLUSION

In this study, a previously developed CFD modeling method, which solved the transient phenomenon of the ceiling fan's rotation with steady-state simulations using a rotation reference frame, was used to investigate the ceiling fan's influence on UR-UVGI disinfection efficacy. Two air exchange rates, 2 and 6 ACH, and four fan downward rotational speeds, 0, 80, 150, 235 rpm, were considered in this study. The investigation used the UV dose to represent the disinfection of microorganisms, and the indices, including the fraction of remaining microorganisms, equivalent air exchange rate, UR-UVGI effectiveness and TB infection probability, to assess the system performance. According to the simulation results, the ambient air exchange rate was a decisive factor in determining the UR-UVGI disinfection efficacy. This is a little misleading in practice, however, because while increased ventilation may reduce the contribution of UR-UVGI, the combined effect of greater ventilation and UR-UVGI is always less, and never greater, risk of infection. Furthermore, the UR-UVGI disinfection efficacy improved with the use of a ceiling fan. However, a high fan speed might not result in better performance than medium or low fan speeds, all of which may approach near perfect mixing. The results for infection probability also indicated the possibility of increasing the TB infection risk by using ceiling fan without effective air disinfection by ventilation, natural or mechanical, or UR-UVGI.

In the future, we plan to apply this CFD modeling method to parametric investigation of ceiling fan's influence on UR-UVGI disinfection efficacy by focusing on the effects of fan rotational direction and speed, microorganisms and heat source conditions, UV fixtures and spatial configuration. Furthermore, as ceiling fans are widely used in the indoor environments with natural ventilation, especially in the resource-limited areas, it is important to investigate the proper application of ceiling fans in the naturally ventilated environments. Most important, we will consider the application of ceiling fans in the real world in the aforementioned investigations, with regard to both thermal comfort and UR-UVGI disinfection efficacy.

Acknowledgements—This study was supported by the Fogarty Grant project "Sustainable Air Design Technology Innovations for Resource Limited Settings" (Grant number: R24TW008821), which was funded under the American Recovery and Reinvestment Act (ARRA) of 2009 by Fogarty International Center, National Institutes of Health, USA. The authors would like to thank Dr. Melvin First in Harvard School of Public Health, who was the main member of the project and passed away in 2011, for his great contribution to the project.

REFERENCES

1. Wells, W. F., M. W. Wells and T. S. Wilder (1942) The environmental control of epidemic contagion I-an epidemiologic study of radiant disinfection of air in day schools. *Am. J. Epidemiol.* **35**(1), 97–121.
2. Riley, R. L. and S. Permutt (1971) Room air disinfection by ultraviolet irradiation of upper air. Air mixing and germicidal effectiveness. *Arch. Environ. Health* **22**, 208–219.
3. Riley, R. L., S. Permutt and J. E. Kaufman (1971) Room air disinfection by ultraviolet irradiation of upper air. Further analysis of convective air exchange. *Arch. Environ. Health* **23**, 35–39.
4. Riley, R. L. and J. E. Kaufman (1972) Effect of relative humidity on the inactivation of airborne *Serratia marcescens* by ultraviolet radiation. *Appl. Microbiol.* **23**(6), 1113–1120.
5. First, M. W., S. N. Rudnick, K. F. Banahan, R. L. Vincent and P. W. Brickner (2007) Fundamental factors affecting upper-room ultraviolet germicidal irradiation-part I. Experimental. *J. Occup. Environ. Hyg.* **4**(5), 321–331. DOI: 10.1080/15459620701271693
6. Rudnick, S. N. and M. W. First (2007) Fundamental factors affecting upper-room ultraviolet germicidal irradiation – part II. Predicting effectiveness. *J. Occup. Environ. Hyg.* **4**(5), 352–362. DOI: 10.1080/15459620701298167
7. Escombe, A. R., D. A. J. Moore, R. H. Gilman, M. Navincopa, E. Ticona, B. Mitchell, C. Noakes, C. Martinez, P. Sheen, R. Ramirez, W. Quino, A. Gonzalez, J. S. Friedland and C. A. Evans (2009) Upper-room ultraviolet light and negative air ionization to prevent tuberculosis transmission. *PLoS Med.* **6**(3), 312–323. DOI: 10.1371/j.pmed.1000043
8. Noakes, C. J., P. A. Sleigh, L. A. Fletcher and C. B. Beggs (2006) Use of CFD modelling to optimise tge design of upper-room UVGI disinfection systems for ventilation rooms. *Indoor Built Environ.* **15** (4), 347–356. DOI: 10.1177/1420326X06067353
9. Sung, M. and S. Kato (2010) Method to evaluate UV dose of upper-room UVGI system using the concept of ventilation efficiency. *Build. Environ.* **45**(7), 1626–1631. DOI: 10.1016/j. buildenv. 2010.01.011
10. Memarzadeh, F., R. N. Olmsted and J. M. Bartley (2010) Applications of ultraviolet germicidal irradiation disinfection in health care facilitiesL effective adjuct, but not stand-alone technology. *Am. J. Infect. Control* **38**(5), S13–S24. DOI: 10.1016/j.ajic.2010.04.208
11. Heidarinejad, M. (2011) *Using Computational Fluid Dynamics (CFD) to Study Upper-Room UVGI Lamp Disinfection Effectiveness in the Patients' Rooms*. M.Sc. thesis, The Pennsylvania State University.
12. Zhu, S., J. Srebric, S. N. Rudnick, R. L. Vincent and E. A. Nardell (2012) *Numerical Approach for Studying Ceiling Fan's Influence on Upper-Room UVGI's Disinfection Efficacy*. Proceedings of the 10th International Conference for Healthy Buildings, Brisbane, Australia, 8–12 July 2012.
13. Kato, S. and J.-H. Yang (2008) Study on inhaled air quality in a personal air-conditioning environment using new scales of ventilation efficiency. *Build. Environ.* **43**(4), 494–507. DOI: 10:1016/j.buildenv. 2006.08.019

14. Wells, W. F. (1955) *Airborne Contagion and Air Hygiene: An Ecological Study of Droplet Infection*. Harvard University Press, Cambridge, MA.
15. Riley, E. C., G. Murphy and R. L. Riley (1978) Airborne spread of measles in a suburban elementary school. *Am. J. Epidemiol.* **107**(5), 421–432.
16. CD-adapco (2011) User Guide of STAR-CCM+ 6.04.014. CD-adapco, Melville, NY.
17. Shih, T.-H., W. W. Liou, A. Shabbir, Z. Yang and J. Zhu (1994) A new k-ε eddy viscosity model for high Reynolds number turbulent flows-model development and validation. *Comput. Fluids* **24**(3), 227–238. DOI: 10.1016/0045-7930(94)00032-T
18. Patankar, S. V. (1980) Calculation of the flow field. In *Numerical Heat Transfer and Fluid Flow* (Edited by M. A. Phillips and E. M. Millman), pp. 113–138. McGraw-Hill Book Company, New York, NY.
19. Rodi, W. (1991) *Experience With Two-Layer Models Combining the k-e Model With A One-Equation Model Near the Wall. 13, AIAA*, Proceedings of 29th Aerospace Sciences Meeting, Reno, NV, 7–10 January 1991.
20. Wolfstein, M. (1969) The velocity and temperature distribution in one-dimensional flow with turbulence augmentation and pressure gradient. *Int. J. Heat Mass Transfer.* **12**(3), 301–318. DOI: 10.1016/0017-9310(69)90012-X
21. Kato, S., K. Ito and S. Murakami (2003) Analysis of visitation frequency through particle tracking method based on LES and model experiment. *Indoor Air* **13**(2), 182–193. DOI: 10.1034/j.1600-0668.2003.00173.x
22. Samdberg, M. (1983) The use of moments for ventilation assessing air quality in ventilated room. *Build. Environ.* **18**(4), 181–197. DOI: 10:1016/0360-1323(83)90026-4
23. Davidson, L. and E. Olsson (1987) Calculation of age and local purging flow rate in rooms. *Build. Environ.* **22**(2), 111–127. DOI: 10:1016/0360-1323(87)90031-X
24. Rudnick, S. N., M. W. First, T. Sears, R. L. Vincent, P. W. Brickner, P. Y. Ngai, J. Zhang, R. E. Levin, K. Chin, R. O. Rahn, S. L. Miller and E. A. Nardell (2012) Spatial distribution of fluence rate from upper room ultraviolet germicidal irradiation: Experimental validation of a computer-aided design tool. *HVAC&R Res.* **18**(4), 774–794. DOI: 10.1080/10789669.2012.667863
25. Kato, S. and S. Murakami (1992) New scales for ventilation efficiency and their application based on numerical simulation of room airflow, pp. 22–37. The University of Tokyo, Proceedings of International Symposium on Room Air Convection and Ventilation Effectiveness, Tokyo, Japan, 22–26 July 1992.
26. NIOSH (2009) *Environmental Control for Tuberculosis: Basic Upper-Room Ultraviolet Germicidal Irradiation Guidelines for Healthcare Settings*. Centers for Disease Control and Prevention, National Institute for Occupational Safety and Health, Washington, DC.
27. Novoselac, A. and J. Srebric (2003) Comparison of air exchange efficiency and contaminant removal effectiveness as IAQ indices. *ASHRAE Trans.* **109**(2), 339–349.
28. Zhu, S., J. Srebric, J. D. Spengler and P. Demokritou (2012) An advanced numerical model for the assessment of airborne transmission of influenza in bus microenvironments. *Build. Environ.* **47**(4), 67–75. DOI: 10:1016/j.buildenv.2011.05.003
29. Wood, R., S. Johnstone-Robertson, P. Uys, J. Hargrove, K. Middelkoop, S. D. Lawn and L. G. Bekker (2010) Tuberculosis transmission to young children in a South African community: modeling household and community infection risks. *Clin. Infect. Dis.* **51**(4), 401–408. DOI: 10.1086/655129
30. Nishi, Y., A. Miyazaka, T. Horikosi, A. Ishii, H. Hanzawa, T. Tsuchikawa, Y. Kurazumi, S. Tanabe, S. Tamura and N. Kakitusba (2005) Human and thermal environment. In *Mechanism of Comfortable Thermal Environment* (Edited by Y. Nishi), p. 30. Maruzen, Japan.